

Domain structure of a $\text{Nd}_{60}\text{Al}_{10}\text{Fe}_{20}\text{Co}_{10}$ bulk metallic glass

Bing Chen Wei, Wei Hua Wang,* and Ming Xiang Pan

National Microgravity Laboratory, Institute of Mechanics, and Institute of Physics and Center for Condensed Matter Physics, Chinese Academy of Sciences, Beijing 100080, China

Bao Shan Han and Zhen Rong Zhang

State Key Laboratory of Magnetism, Institute of Physics and Center for Condensed Matter Physics, Chinese Academy of Sciences, Beijing 100080, China

Wen Rui Hu

National Microgravity Laboratory, Institute of Mechanics, Chinese Academy of Sciences, Beijing 100080, China

(Received 27 February 2001; published 8 June 2001)

Magnetic domain structure of $\text{Nd}_{60}\text{Al}_{10}\text{Fe}_{20}\text{Co}_{10}$ bulk metallic glass (BMG) has been studied by using magnetic-force microscopy. In the magnetic-force images it is shown that the exchange-interaction-type magnetic domains with a period of about 360 nm do exist in the BMG, which is believed to be associated with the appearance of hard-magnetic properties in this system. The existence of the large-scale domains demonstrates that the magnetic moments of a great deal of short-scale ordered atomic clusters in the BMG have been aligned by exchange coupling. Annealing at 715 K leads to partial crystallization of the BMG. However, the exchange coupling is stronger in the annealed sample, which is considered to arise from the increase of transition-metal concentration in the amorphous phase due to the precipitation of Nd crystalline phase.

DOI: 10.1103/PhysRevB.64.012406

PACS number(s): 75.50.Kj, 61.43.Dq, 75.70.Kw, 81.05.Kf

Nd-Fe-Al-based bulk metallic glasses (BMG) with a diameter up to 12 cm have been recently prepared.¹ This BMG system has evoked an extensive attention due to its hard magnetic properties at room temperature.²⁻⁸ The high coercivity of these amorphous alloys is striking because no structural anisotropy exists in the disordered packing solid. It is supposed that the BMG is an ensemble of short-scale ordered magnetic atomic clusters in uniform distribution. These clusters consist of Nd and transition elements and possess large random anisotropy. It is the magnetic-exchange coupling among them that causes the high coercivity of this magnetic system. Most of the consequent results supported this model.⁷⁻⁹ However, no direct experimental evidence for the existence of exchange-coupling interaction in this system has been presented so far. Therefore, it is of a special interest to study the magnetic domain structure of the BMG. In this paper, the magnetic domain structure of $\text{Nd}_{60}\text{Al}_{10}\text{Fe}_{20}\text{Co}_{10}$ was investigated by magnetic-force microscopy (MFM).

Ingots with compositions of $\text{Nd}_{60}\text{Al}_{10}\text{Fe}_{20}\text{Co}_{10}$ were prepared by arc melting from elemental Nd, Fe, Al, and Co with a purity of 99.9% in a titanium-gettered argon atmosphere. Cylindrical specimens of around 3 mm in diameter and 50 mm in length were prepared from the ingots by die casting into a copper mold under argon atmosphere. The details of preparation can be seen in Ref. 5. The structure of the as-cast cylinder was characterized by x-ray diffraction (XRD).⁵ Magnetic measurements were performed using a vibrating sample magnetometer with a maximum applied field of 1592 kA m^{-1} . The study of domain structure was carried out by using Digital Instruments NanoScope IIIa D-3000 MFM. It allows the topographic and magnetic-force images to be collected separately and simultaneously in the same area of the sample by using Tapping/Lift modes. The magnetic tips used were microfabricated Si cantilevers with a pyramidal tip

coated with magnetic Co-Cr thin film of 40 nm thickness and a coercivity of about 32 kA m^{-1} . For the mode of dynamic detection, the cantilever is vibrated and its resonant frequency f_0 and phase ϕ will be modulated by the magnetic forces exerted on the tip from the stray field H emerged from the magnetic structures in the sample surface layer when the tip is scanning. In fact, for the phase detection, the phase shift ΔQ can be written as $\Delta\phi = QF'/k$, where F' is the vertical (z) component of the force gradient, k and Q are the spring constant and the quality factor of the cantilever, respectively. In the point-dipole approximation, if the tip is vertically magnetized, $F' = m_z \partial^2 H_z / \partial z^2$, where m_z is the magnetic moment of the tip and H_z is the vertical component of H . In the magnetic-force images detected by the phase mode, the dark and bright regions correspond to the attractive and repulsive tip-sample interactions, respectively. In our experiment, the tip used was magnetized upward prior to imaging. Its $f_0 = 80.6$ kHz, and its lift-height during scanning was 30 nm. The samples for MFM study were fresh cut from the same cylinder. After grinding and polishing, they were vacuum annealed at 453 K for 36 ks to remove the stress built in the surface layer.

The as-cast cylinder exhibits an XRD spectrum typical for amorphous phase without obvious crystalline reflection peaks. Figure 1 shows the dependence of coercivity H_c , saturation magnetization M_s , and remanence M_r on isothermal annealing temperature for the $\text{Nd}_{60}\text{Al}_{10}\text{Fe}_{20}\text{Co}_{10}$ BMG. The inset exhibits its hysteresis loop at room temperature. It is shown that the as-cast $\text{Nd}_{60}\text{Al}_{10}\text{Fe}_{20}\text{Co}_{10}$ BMG exhibits H_c of 326 kA m^{-1} , M_s of 10.8 $\text{A m}^2 \text{kg}^{-1}$, and M_r of 7.2 $\text{A m}^2 \text{kg}^{-1}$. These values are consistent with the previous results of Nd-Fe-Al-based BMG's,^{2,6-8} indicating that the BMG is a permanent magnetic material with relative high coercivity and rather low magnetization compared with the

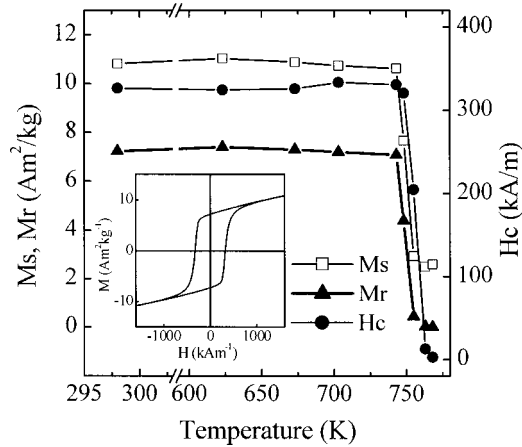


FIG. 1. Dependence of H_c , M_s , and M_r on isothermal annealing temperature for $\text{Nd}_{60}\text{Al}_{10}\text{Fe}_{20}\text{Co}_{10}$ alloy (annealing for 1.8 ks). The inset shows the hysteresis loop at room temperature.

nanocomposite rare-earth permanent magnets. The hard magnetic properties remain almost unchanged in the annealing-temperature range from room temperature up to 740 K, and disappear after full crystallization of the BMG above 760 K.^{6,9} The presence of only one magnetic phase in the as-cast cylinders was confirmed by the curve of magnetization vs temperature, in which only one magnetic transition appears at Curie temperature of about 470 K before crystallization. The above results have demonstrated that the hard magnetic properties of the Nd-Fe-Al-based BMG's are presented by the amorphous phase instead of the crystallized one. This is also confirmed by other work.^{2,6-8}

MFM was employed to image the magnetic domain structure in this BMG. Obvious magnetic contrast was observed in the magnetic-force images. In order to verify the reliability of these images the samples were rescanned under same experimental conditions and the practically identical images as its first scanning were obtained. For the as-cast BMG, a typical (10×10)- μm magnetic-force image is shown in Fig. 2(a). It can be seen that the image is characterized by darker areas adjacent with brighter areas in submicron scale and in random distribution. Higher magnification images from the as-cast sample did not provide additional detail. In fact, the dark area indicates that the magnetization direction in this area is nearly parallel to the upward tip magnetization, and the bright area indicates the opposite. This kind of magnetic contrast is similar to the so-called "exchange-coupling domains" presented in the nanocomposite rare-earth-transition-metal permanent materials, in which strong exchange-coupling interaction exists between hard and soft magnetic grains.¹⁰⁻¹³ The average period T of the domain pattern and the average contrast between dark and bright areas were measured by means of section analysis. A large number of sections were analyzed in order to get statistical results. A typical section analysis of $\Delta\phi$ vs the length of the section is shown in Fig. 2(b). It can be seen that the average roughness $(Ra)_{\Delta\phi}$ and root mean square $(Rms)_{\Delta\phi}$ describing the contrast of the image are 0.94° and 0.72° , respectively, and $T = 360 \text{ nm}$.

According to the cluster model of the Nd-Fe melt-

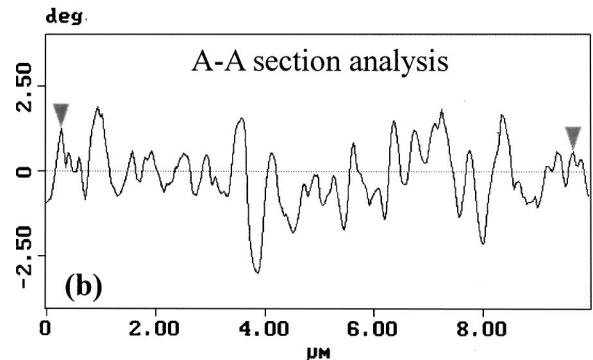
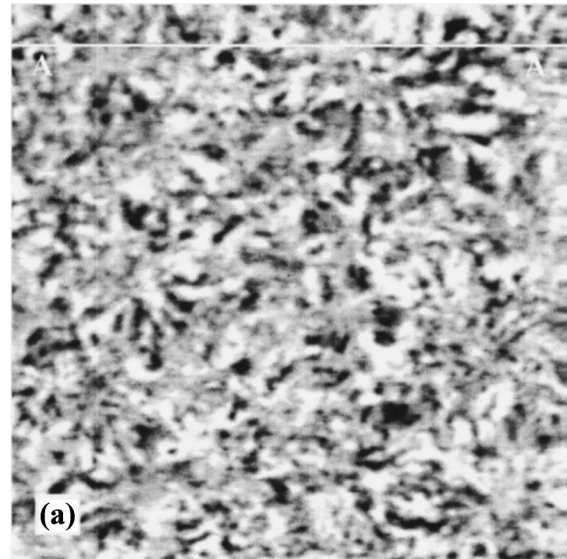


FIG. 2. Magnetic-force image with a scan size $10 \times 10 \mu\text{m}$ for the as-cast $\text{Nd}_{60}\text{Al}_{10}\text{Fe}_{20}\text{Co}_{10}$ BMG (a), and typical section-analysis result (b).

spinning magnetic system, the exchange-coupling interaction among magnetic clusters with random anisotropy could cause the high coercivity of the magnetic system.^{14,15} Inoue, Takeuchi, and Zhang confirmed the presence of these short-range ordered clusters in the Nd-Fe-Al-system BMG by high-resolution transmission-electron microscopy and radial distribution-function studies.² Xing *et al.* and Fan *et al.* have estimated the size of the clusters to be nearly 2 nm.^{7,8} In the present study, the as-cast BMG exhibits a typical amorphous pattern without obvious crystalline-reflection peaks. This gives an upper limit of a few nanometers for the cluster size. However, the above section analysis of the magnetic-force images of the $\text{Nd}_{60}\text{Al}_{10}\text{Fe}_{20}\text{Co}_{10}$ BMG has shown that their magnetic domains are in submicron scale, which is significantly larger than the size of the ordered atomic clusters composed of the Nd-Fe and Nd-Co atoms. We infer that it is the experimental evidence of the existence of strong exchange coupling. It is by the exchange coupling that a great deal of short-scale ordered atomic clusters are aligned to form the large-scale domains. In other words, the large areas of magnetic contrast are actually a collection of a group of clusters with similar magnetic orientation aligned by exchange coupling. Furthermore, the presence of strong exchange coupling is also confirmed by the significant rema-

nence enhancement of our BMG. Its M_r/M_s value is 0.67, which is obviously greater than 0.5, the value predicted for randomly oriented and noninteracting particles by the Stoner-Wohlfarth theory.¹³ Considering that the dimension of the ordered magnetic clusters of the present hard magnetic material has to be larger than the exchange length according to the random-anisotropy model, the number of clusters in one group could be estimated as 10^3-10^4 .¹⁶

The magnetic-force image of the sample annealed at 715 K for 1800 s is shown in Fig. 3(a). The exchange-coupling domains are also observed. However, there exist a number of large gray (nonmagnetic) areas in this annealed sample, which actually correspond to the large round particles in the topographic image. Electron microscopy and composition analysis have shown that these grains with size of 1–2 μm are of paramagnetic pure Nd crystalline phase.⁹ Moreover, although the magnetic structure in the region apart from these nonmagnetic areas is similar to the as-cast sample, the contrast of the domain and T become larger in the annealed sample. The statistical results measured from typical section analysis [Fig. 3(b)] are $(Ra)_{\Delta\phi} = 1.15^\circ$, $(\text{rms})_{\Delta\phi} = 0.88^\circ$, and $T = 0.42 \mu\text{m}$. Annealing at 715 K give rise to the precipitation of the paramagnetic Nd crystals from the amorphous matrix. The precipitation of the paramagnetic phase will decrease the magnetization of the system. On the other hand, the precipitation of Nd will enrich the concentration of transition metals in the remaining amorphous phase, and thereby increase M_s due to a stronger exchange-coupling interaction among the magnetic clusters in the remainder. This can be confirmed by the increased size of domain contrast and domain period in the annealed sample as shown in Figs. 3(a) and 3(b). Consequently, the conjunct effect of these two factors leads to the almost unchanged M_s after annealing at temperature below 740 K (Fig. 1). Similarly, the annealing should increase the size of the clusters D by a certain degree. This will cause the decrease of coercivity according to the well-known $1/D$ dependence.¹⁷ At the same time the precipitation of the crystalline phase in the amorphous matrix plays a role in pinning the domain walls. As a result, the coercivity also remains unchanged prior to full crystallization (Fig. 1).

In conclusion, the presence of exchange coupling interaction between a great deal of short-scale ordered magnetic atomic clusters in $\text{Nd}_{60}\text{Al}_{10}\text{Fe}_{20}\text{Co}_{10}$ BMG is experimentally confirmed by the magnetic-force images. The exchange-

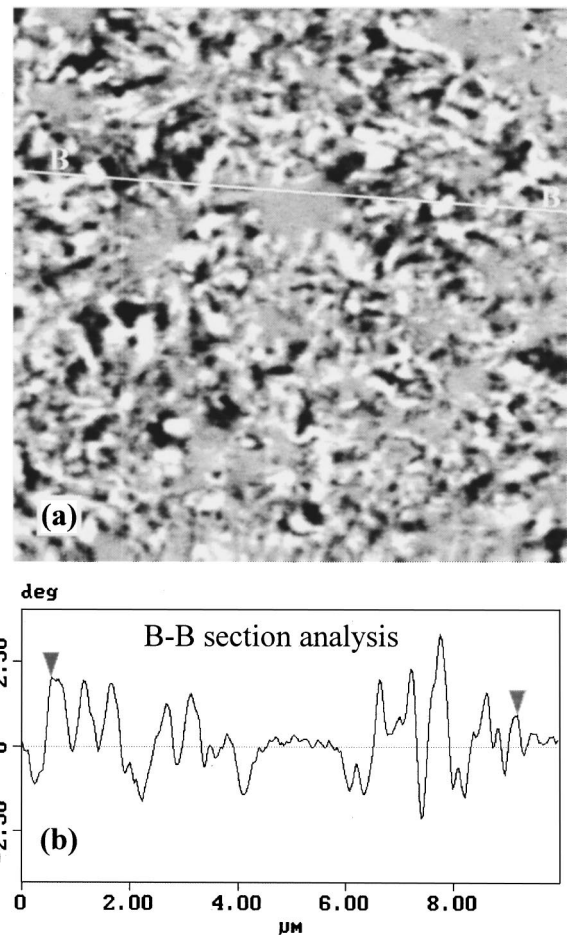


FIG. 3. Magnetic-force image with a scan size $10 \times 10 \mu\text{m}$ for the $\text{Nd}_{60}\text{Al}_{10}\text{Fe}_{20}\text{Co}_{10}$ BMG annealed at 715 K for 1.8 ks (a), and typical section-analysis result (b).

coupling domains shed light on the appearing of macroscopic hard magnetic properties in the BMG. The magnetic domains have a length scale of about 360 nm, and are composed of a group of magnetic clusters aligned by exchange coupling.

This work was supported by the National Natural Science Foundation of China (Grants Nos. 59925101 and 50031010).

*Author to whom correspondence should be addressed. Electronic address: whw@aphy.iphy.ac.cn

¹A. Inoue, T. Zhang, A. Takeuchi, and W. Zhang, *Mater. Trans., JIM* **37**, 636 (1996).

²A. Inoue, A. Takeuchi, and T. Zhang, *Metall. Mater. Trans. A* **29A**, 1779 (1998).

³A. Inoue, *Acta Mater.* **48**, 279 (2000).

⁴Y. Li, S. C. Ng, Z. P. Lu, Y. P. Feng, and K. Lu, *Philos. Mag. Lett.* **78**, 213 (1998).

⁵B. C. Wei, Y. Zhang, Y. X. Zhuang, D. Q. Zhao, M. X. Pan, W. H. Wang, and W. R. Hu, *J. Appl. Phys.* **89**, 3529 (2001).

⁶X. Z. Wang, Y. Li, J. Ding, L. Si, and H. Z. Kong, *J. Alloys Compd.* **290**, 209 (1999).

⁷L. Q. Xing, J. Eckert, W. Löser, S. Roth, and L. Schultz, *J. Appl. Phys.* **88**, 3565 (2000).

⁸G. J. Fan, W. Loser, S. Roth, J. Eckert, and L. Schultz, *Appl. Phys. Lett.* **75**, 2984 (1999).

⁹B. C. Wei, W. H. Wang, D. Q. Zhao, Y. Zhang, P. Wen, M. X. Pan, and W. R. Hu, *Sci. China, Ser. A: Math., Phys., Astron.* **44**, 790 (2001).

¹⁰L. Folks and R. C. Woodward, *J. Magn. Magn. Mater.* **190**, 28 (1998).

¹¹M. A. Al-Khafaji, W. M. Raiforth, M. R. J. Gibbs, H. A. Davies, and J. E. L. Bishop, *J. Magn. Magn. Mater.* **182**, 111 (1998).

¹²M. A. Al-Khafaji, W. M. Raiforth, M. R. J. Gibbs, H. A. Davies, and J. E. L. Bishop, *J. Magn. Magn. Mater.* **188**, 109 (1998).

- ¹³M. A. Al-Khafaji, S. P. H. Marashi, W. M. Raiforth, M. R. J. Gibbs, H. A. Davies, J. E. L. Bishop, and G. Heydon, *J. Magn. Mater.* **190**, 48 (1998).
- ¹⁴K. Siratori, K. Nagayama, H. Ino, N. Saito, and Y. Nakagawa, *J. Phys. Soc. Jpn.* **59**, 2483 (1990).
- ¹⁵R. C. Taylor, T. R. McGuire, J. M. D. Coey, and A. Gangulee, *J. Appl. Phys.* **49**, 2885 (1978).
- ¹⁶R. Alben, J. J. Becker, and M. C. Chi, *J. Appl. Phys.* **49**, 1653 (1978).
- ¹⁷F. Pfeifer and C. Radeloff, *J. Magn. Mater.* **19**, 190 (1980).